An ultrahigh-Q silicon racetrack resonator based on multimode waveguide bends

Zihan Zhang
State Key Laboratory of Advanced Optical Communication Systems and Networks, Department of Electronic Engineering, Shanghai Jiao Tong University, Shanghai 200240, China
zihanzhang@sjtu.edu.cn

Lu Sun*
State Key Laboratory of Advanced Optical Communication Systems and Networks, Department of Electronic Engineering, Shanghai Jiao Tong University, Shanghai 200240, China
*Corresponding author
sunlu@sjtu.edu.cn

Rui Hu
State Key Laboratory of Advanced Optical Communication Systems and Networks, Department of Electronic Engineering, Shanghai Jiao Tong University, Shanghai 200240, China
rui_hu@sjtu.edu.cn

Qiyao Sun
State Key Laboratory of Advanced Optical Communication Systems and Networks, Department of Electronic Engineering, Shanghai Jiao Tong University, Shanghai 200240, China
sqy_sqy@sjtu.edu.cn

Yingdi Pan
State Key Laboratory of Advanced Optical Communication Systems and Networks, Department of Electronic Engineering, Shanghai Jiao Tong University, Shanghai 200240, China
sevens@sjtu.edu.cn

Yikai Su
State Key Laboratory of Advanced Optical Communication Systems and Networks, Department of Electronic Engineering, Shanghai Jiao Tong University, Shanghai 200240, China
yikaisu@sjtu.edu.cn

2023 Opto-Electronics and Communications Conference (OECC) | 978-1-6654-6213-6/23/$31.00 ©2023 IEEE | DOI: 10.1109/OECC56963.2023.10209665

***Abstract*— An ultrahigh-*Q* compact silicon racetrack resonator based on multimode waveguide bends (MWBs) is proposed and demonstrated. The MWB is defined by a combination of cubic and circular curves. The free spectral range (FSR) is measured to be 0.96 nm with an intrinsic *Q*-factor as high as 1.99×10^6.**

Keywords—Ultrahigh-Q, silicon racetrack resonator, multimode waveguide bend

I. Introduction

In the past decades, silicon photonics has grown rapidly and shown great potential in optical communication systems because of its good performance and compatibility with complementary metal-oxide semiconductor (CMOS) process [1]. For example, compact silicon micro-ring resonators (MRRs) with ultrahigh-Q factors have been widely used in microwave filters [2], lasers [3], and sensors [4]. However, the Q-factors are limited by the scattering losses induced by the waveguide sidewall roughness which are inevitable due to fabrication imperfections. Great efforts had been made to realize the high-Q MRRs. A ring resonator with a Q-factor as high as 2.2×10^7 was realized by using thick silicon ridge waveguide [5]. However, the corresponding free spectral range (FSR) is only 0.043 nm with the radius of the ring being as large as 2.45 mm, which limits the application of the resonator. By using waveguide tapers to connect straight multimode ridge waveguides and 180° single-mode ridge waveguide bends, FSR up to 0.325 nm was achieved with the resonator length reduced to 2025 μm [6]. However, it is quite challenging to further reduce the footprint of resonator because long waveguide tapers are needed to avoid intermodal crosstalk in the waveguide bends. To solve this problem, an ultrahigh-Q MRR using strip waveguides was proposed [7]. Multimode waveguide bends (MWBs) defined by modified Euler curves were adopted to replace the single-mode bends. The mode mismatch at the connections between the multimode straight waveguides (MSWs) and MWBs is minimized to suppress the intermodal crosstalk. The whole device is very compact, showing a FSR of 0.9 nm and a Q-factor of 2.3×10^6. Nevertheless, ultrahigh-Q MRRs with larger FSRs or equivalently more compact footprints are still demanded.

In this paper, we propose and demonstrate an ultrahigh-Q racetrack ring which consists of two MSWs and two MWBs. The trajectory of the bends is chosen to be a combination of cubic and circular curves so as to minimize the intermodal crosstalk. The FSR of the MRR is measured to be 0.96 nm while the intrinsic Q-factor is as high as 1.99×10^6. The corresponding propagation loss of the multimode waveguide is therefore 0.33 dB/cm.

II. Design and Simulations

Figure 1(a) shows the schematic configuration of a 180° MWB, which is made up of three parts: a 30° lower bend, a 120° middle arc, and a 30° upper bend. The lower bend is described by a cubic polynomial curve as follows:

$$y = \frac{x^3}{6C} \tag{1}$$

where C is the parameter that determines the size and shape of the bend. The upper 30° bend and the lower 30° bend are mirror-symmetric counterparts and connected by a 120° arc. R which represents the radius of the arc is chosen to be 14.7 μm. The effective radius R_{eff} of the bend is defined as the radius of a semicircle with the same perimeter as the proposed 180° bend. It is calculated to be 23.4 μm in our case. The MWB has a width of 1.6 μm and can support four transverse electric (TE) modes. The form factor C is set as 371.2 in order to increase the curvature from nearly zero to $1/R$. The approximately zero curvature matches that of the MSWs to minimize the mode mismatch at the MWB-MSW junction. The continuously varying curvature gradually convert the modal fields in MSWs to those in MWBs with negligible losses. To verify the suppression of the intermodal crosstalk in this structure, we simulate the light propagation in the MWB using 3D-FDTD methods when TE_0 mode is launched from the lower input end. As shown in Figure 1(b), the excess loss of TE_0 mode is less than 0.05 dB and the intermodal crosstalk of TE_1 - TE_3 modes is below -32.7 dB in the wavelength range of 1500 - 1600 nm. The numerical results prove that higher-order modes are well suppressed in the MWB and no significant mode mismatch would emerge at the interface between the MWB and the MSW. Therefore, we can use the proposed 180° MWB to construct the racetrack ring resonator with very low intermodal crosstalk.

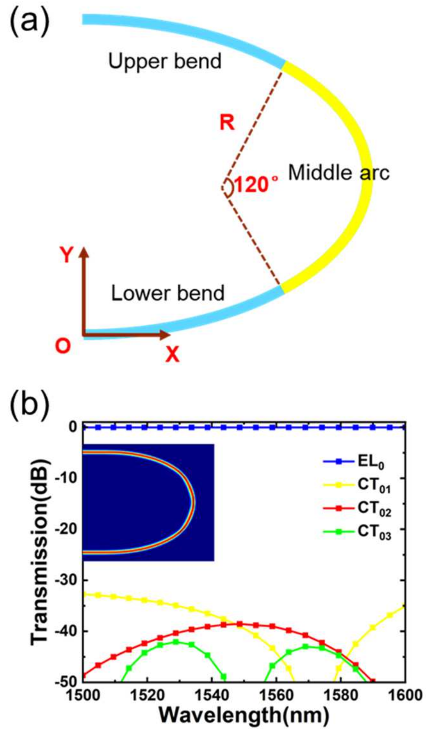

Fig. 1. (a) Schematic diagram of the 180° MWB, which is composed of a pair of 30° cubic-curve bends and a 120° arc. (b) Simulated transmission spectra of the 180°MWB with different mode inputs (TE_0-TE_3). The inset shows the propagation profile of the fundamental mode in the MWB.

Figures 2(a) and 2(b) show the 3D view and the top view of the proposed silicon racetrack resonator coupled to a single-mode access waveguide. The racetrack resonator consists of two 180° MWBs connected by two MSWs. The resonator is designed based on the silicon-on-insulator (SOI) platform with a 220-nm-thick silicon top layer, a 1-μm-thick upper cladding silica layer and a 2-μm-thick buried oxide layer. We choose the length of MSW L to be 260 μm. The widths of the multimode waveguide W_m and the single-mode waveguide W_s are 1.6 μm and 0.63 μm, respectively. The gap between the micro-ring and the access waveguide W_g is set as 190 nm. They compose the coupling region of the MRR which is a 90° bent directional coupler with the inner radii R and out radii R_c being 14.7 μm and 16.2 μm, respectively. The parameters are designed so as to reach the phase matching condition between the fundamental modes in the narrow and wide waveguides. In this way, only the fundamental mode can be excited in the MRRs when TE_0 mode is launched from the access waveguide.

III. Fabrication and Measurements

The whole device including the racetrack resonator, the access waveguide, and the grating couplers was fabricated with standard 220-nm-SOI multi-project wafer (MPW) processes provided by the CUMEC foundry (United Microelectronics Center, China). Figure 3(a) shows the microscope picture of the fabricated device. The enlarged view of the coupling region is shown in Figure 3(b).

In the measurements, the TE-polarized light from a tunable laser (Santec TSL-770) was coupled into and out of the chip by grating couplers. An optical power meter and a photodetector (Santec MPM-210) were employed for

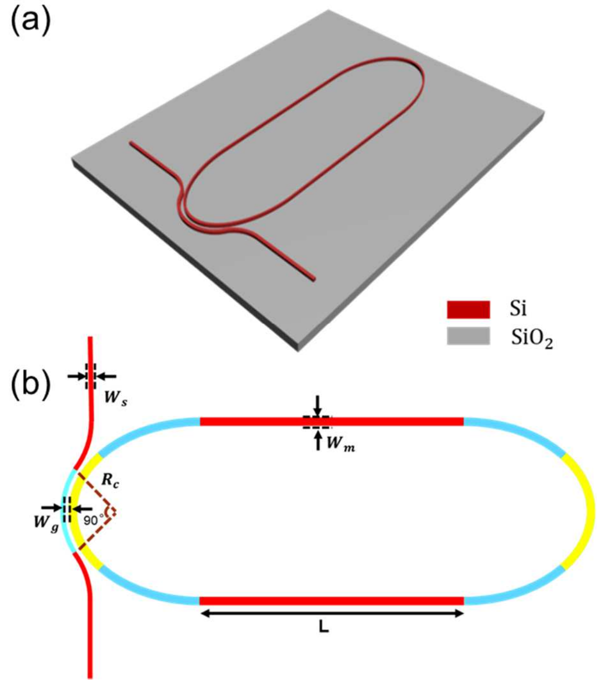

Fig. 2. (a) 3D view and (b) top view schematics of the proposed MRR coupled to a single-mode access waveguide.

optical calibration and receiving the transmitted power, respectively. Figure 4(a) shows the measured spectral response of the MRR. There is only one FSR of 0.96 nm, indicating that only the fundamental mode propagates in the MRR and higher-order modes are successfully suppressed. The Lorenz fit of the major resonance at the wavelength of 1550 nm is shown in Figure 4(b). The 3-dB bandwidth is about $\Delta\lambda = 1.43$ pm, which corresponds to a loaded Q-

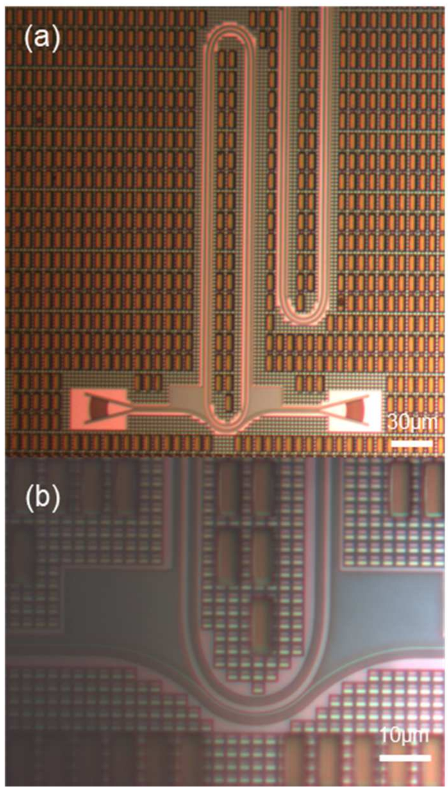

Fig. 3. Microscope picture of the fabricated device. (a) Top view of the whole device and (b) enlarged view of the coupling region.

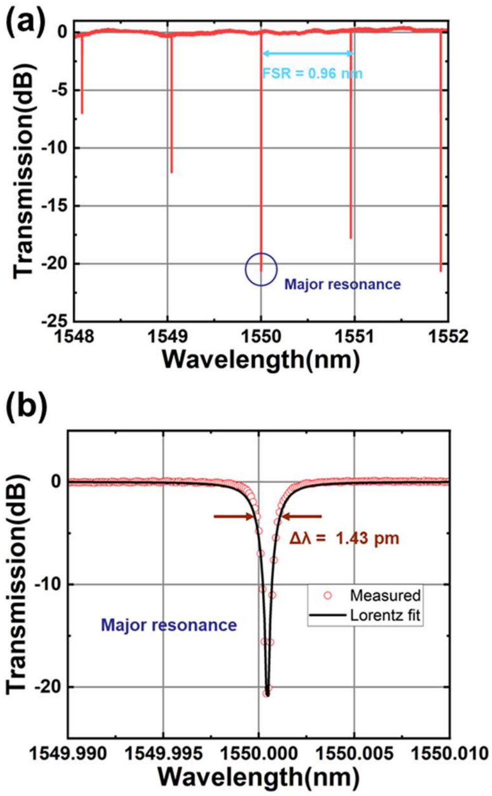

Fig.4. (a) Transmission spectrum of the MRR in the wavelength range of 1548 - 1552 nm. The FSR is 0.96 nm. (b) Lorentz fit of the major resonance at the wavelength of 1550 nm.

factor of 1.09×10^6. The extinction ratio is 20.87 dB. Hence, the intrinsic Q-factor is as high as 1.99×10^6, which means the propagation loss of the multimode waveguide is as low as 0.33 dB/cm. Table I shows the reported ultrahigh-Q MRRs with Q-factors over a million in recent years. As far as we know, the proposed racetrack resonator has the largest FSR among the silicon MRRs with Q-factors over 10^6 as a result of the very compact footprint. The FSR can be further increased by reducing the lengths of the MSWs composing the racetrack resonator, which leads to many benefits such as providing more channels in a wavelength division multiplexing (WDM) system.

TABLE I. STATE-OF-THE-ART SILICON MRRS WITH Q-FACTORS OVER A MILLION

Ref.	Waveguide	R_{eff} (μm)	FSR(nm)	$Q_{intrinsic}$
[5]	Ridge	2450	0.043	2.2×10^7
[6]	Ridge	70	0.325	2.7×10^6
[7]	Strip	29	0.900	2.3×10^6
This work	Strip	23.4	0.960	1.99×10^6

IV. CONCLUSION

In summary, we proposed and experimentally demonstrated an ultrahigh-Q and compact racetrack resonator based on MWBs. By employing a combination of cubic and circular curves as the waveguide trajectory, the MWB shows negligible bending losses and intermodal crosstalk. It was then used to construct a racetrack resonator in which the fundamental mode propagation can be maintained. The fabricated MRR has a measured FSR of 0.96 nm. The loaded and intrinsic Q-factors are 1.09×10^6 and 1.99×10^6, respectively. The proposed racetrack ring resonator could find applications in a variety of fields including narrow-band filters, low-threshold lasers, highly sensitive sensors, etc.

ACKNOWLEDGMENT

This work was supported in part by National Key Research and Development Program of China (2019YFB2203503), and National Natural Science Foundation of China (62035016, 62105200, 61835008, 61860206001).

REFERENCES

[1] D. Thomson et al, “Roadmap on silicon photonics,” J. Opt., vol. 18, no. 7, pp. 1-20, 2016.

[2] M. S. Rasras et al, “Demonstration of a tunable microwave-photonic notch filter using low-loss silicon ring resonators,” J. Lightwave Technol., vol. 27, pp. 2105-2110, 2009.

[3] B. Stern, J. Xingchen, A. Dutt, and M. Lipson, “Compact narrow-linewidth integrated laser based on a low-loss silicon nitride ring resonator,” Opt. Lett., vol. 42, pp. 4541–4544, 2017.

[4] B. Q. Su, C. X. Wang, Q. Kan, and H. D. Chen, “Compact silicon-on-insulator dual-microring resonator optimized for sensing,” J. Lightwave Technol., vol. 29, pp. 1535–1541, 2017.

[5] A. Biberman, M. J. Shaw, E. Timurdogan, J. B. Wright, and M. R. Watts, “Ultralow-loss silicon ring resonators,” Opt. Lett., vol. 37, pp. 4236– 4238, 2012.

[6] H. Qiu et al, “A continuously tunable sub-gigahertz micro-wave photonic bandpass filter based on an ultra-high-Q silicon microring resonator,” J. Lightwave Technol., vol. 36, pp. 4312–4318, 2018.

[7] L. Zhang et al, “Ultrahigh-Q silicon racetrack resonators,” Photonics Res., vol. 8, no. 5, pp. 684-689, 2020.